Thesis for the Degree of Master of Engineering

Laminar Lifted Methane Jet Flames in Co-flow Air Diluted with Helium and Nitrogen

by
Narayan Pandurang Sapkal
Department of Mechanical Engineering
The Graduate School
Pukyong National University

February 22, 2016

Laminar Lifted Methane Jet Flames in Co-flow Air Diluted with Helium and Nitrogen

(헬륨과 질소가 희석된 공기 동축류에서의 층류 메탄 부상화염)

Advisor: Prof. Jeong Park

by

Narayan Pandurang Sapkal

A thesis submitted in partial fulfillment of the requirements for the degree of Master of Engineering in Department of Mechanical Engineering, The Graduate School, Pukyong National University

February 2016

Narayan Pandurang Sapkal의
공학석사 학위논문을 인준함.

2016년 2월

주 심 공학박사 권 오 붕 印

위 원 공학박사 박 정 印

위 원 공학박사 이 창 용 印

Contents

Nomenclature

D	Nozzle diameter
H_L	Liftoff height
H_{free}	Length of the developing region
U_O	Fuel nozzle exit velocity
V_{CO}	Co-flow velocity
$X_{F,O}$	Initial fuel mole fraction
S_L	Stoichiometric un-stretched non-adiabatic laminar burning velocity
r^*_{cur}	Radius of curvature
A^o	Angstrom
v	Kinematic viscosity
R	Correlation coefficient
g	Gravitational acceleration
ρ	Density of gases
Sc	Schmidt number
Ri	Richardson number
Le	Lewis number

Laminar Lifted Methane Jet Flames in Co-flow air Diluted with Helium and Nitrogen

Narayan Pandurang Sapkal

Department of Mechanical Engineering, The Graduate School,
Pukyong National University

Abstract

Lifted flames in laminar jets of methane diluted with helium and nitrogen issuing into a coaxial co-flow air have been investigated experimentally. The chemiluminescence intensities of OH^*, CH_2O^* radicals and the radius of curvature for tri-brachial flame were measured using an intensified charge coupled device (ICCD) camera, monochromator and digital video camera. The product of the OH^* and CH_2O^* is used as a marker for heat release rate. Such methane jet flames could be lifted in buoyancy dominated and jet momentum dominated regimes despite the Schmidt number less than unity. The lifted flames were also stabilized due to buoyancy induced convection in buoyancy-dominated regime causing an increase of reactant mass flux to edge flame and thereby increasing the reaction rate and subsequently edge flame speed. It was confirmed that increased OH^* and CH_2O^* concentration caused an increase of edge flame speed via enhanced chemical reaction in buoyancy-dominated regime. In jet momentum dominated regime lifted flames were observed even for nozzle exit velocities much higher than stoichiometric laminar flame speed. An increase in radius of curvature in addition to the increased OH^* and CH_2O^* concentration stabilizes such lifted flames. Based on the stabilization mechanism, detailed discussion on the stabilization of such lifted flames is made.

1. Introduction

Laminar lifted non-premixed free and co-flow jet flames have been studied extensively to clarify the characteristics of flame stabilization and to use the fundamental data in designing industrial burners. These laminar lifted non-premixed jet flames have been widely studied [1-3], in that those can provide target field for development of advanced laminar stretched flamelet model permitting partially premixed mixture at boundary conditions. Such a laminar lifted flame propagates along the stoichiometric contour due to intrinsic nature at its base such that the leading edge consists of a lean and rich premixed flame wings and a trailing diffusion flame, all extending from a single location. Thus, the stabilization mechanism is addressed to the balance between the tri-brachial flame speed and local axial flow velocity [1-2]. The propagation speed of tribrachial flame has also been investigated extensively [3-7], and it has been found that mixture fraction gradient and flow redirection effect resulted from heat release rate are the two dominant factors that influences the propagation speed. The stability analysis [2] has been performed by assuming that the propagation speed is either constant or relatively insensitive to flow conditions [5]. The lifted flame is found to be stable or unstable when the local flow velocity along the stoichiometric contour decreases or increases with the axial distance in laminar free jets, which corresponds to the cases when Schmidt number, Sc of fuel is larger or smaller than unity [2]. Based on cold jet similarity solutions, experimentally it was shown that propane and n-butane fuels (Sc > 1) exhibited stable lifted flames, while no stable lifted flames were observed for methane and ethane fuels (Sc < 1) in free jets [1]. These lifted flames were stabilized

in the far field of a jet when sub-millimeter size nozzle were used. Stationary lifted flames were also observed in propane co-flow jet flames highly diluted with nitrogen when relatively large size nozzle with the diameter d = O (10 mm) was used. Based on the balance mechanism of a triple flame, jet velocity could be scaled with stoichiometric laminar burning velocity.

There were two distinctive lifted flame stabilization modes were identified, in the developing and developed regions of co-flow jets [8]. It has been found that the buoyancy plays an important role for flame stabilization. Also stationary lifted flames for partially premixed or diluted methane were observed in the near field of co-flow jets [9-11]. However, no systematic explanation on the stabilization mechanism was provided. The existence of stationary lifted flame cannot be fully explained based on the previous stability argument, for methane having (Sc < 1) [2]. So in the present study, efforts have been made to find the reasons behind the stationary lifted flames for methane (Sc < 1).

Concurrently, for the lifted flame stabilization in hot co-flow environment, the important chemical role of intermediate species [12] such as, OH*, CH_2O* in laminar lifted flame stabilization (via reduction in ignition delay time) has been investigated. A recent series of experiments conducted on the methane configuration of the burner has made available instantaneous, simultaneous, high resolution images of temperature, OH mole fraction and key precursor, CH_2O [13]. Investigating the behavior of the flame front as defined by regions of peak heat release rate or reaction rate, has been of great interest to experimental combustion researchers. The seminal work of Paul and Najm [14] showed that the product of OH and CH_2O simultaneous LIF images can be used as an excellent proxy for heat release rate in laminar [15-16] premixed flames. The application of the CH_2O-OH technique for use in transient auto-ignition has also been

explored. In that product of OH* and CH_2O* was represented by heat release rate [17]. Also, correlation of edge flame speed to fuel concentration gradient in a propagating triple flame was addressed using the dependency of fuel concentration gradient upon the radius of curvature [3]. Additionally, the tri-brachial flame speed could be sensitively dependent upon many factors such as mixture strength, buoyancy, heat loss and Lewis number [18].

In this regard, the present study is to explore why laminar lifted methane jet flames diluted with helium and nitrogen (Sc < 1) can be stabilized. To check the effect of buoyancy, Richardson number Ri, was evaluated and chemiluminescence intensities of OH* and CH_2O* have been measured by an intensified charge coupled device (ICCD) camera and monochromator at various conditions. Also, the radius of curvature which is one of the main mechanism of the stabilization of tri-brachial flame is measured at various conditions as well.

2. Experimental Procedure

Schematic diagram of experimental set-up is as shown in the Fig. 1, which consists of a co-flow burner, flow controllers and a visualization system. Two co-flow burners used had a central fuel nozzle made of stainless steel with 9.4 mm and 0.95 mm inner diameters and the length is 100 times of the inner diameter for the flow inside to be fully developed. The co-flow air was supplied to the coaxial nozzle with 90.4 mm inner diameter through a glass beads and honeycomb for the velocity to be uniform. The tip of the fuel nozzle protruded 10.3 mm over the honeycomb. A quartz tube with 20 cm length and 90.4 mm inner diameter was placed on the honeycomb, to minimize outside disturbances. The fuel was a pure grade of methane diluted with nitrogen and helium, compressed air was used for the co-flow. A digital video camera (SONY HDR-CX560) which was triggered to capture the image of stationary lifted flame. The liftoff height was measured by the cathetometer. ICCD camera and monochromator were used for visualize the behavior of lifted flame.

2.1 ICCD experiment

To obtain the chemiluminescence intensities of OH* radicals located at flame front, ICCD camera (1024x1024 pixels, Princeton Instrument, PI-MAX4) was used. A TECHSSPEC bandpass filter of bandwidth 10 nm, center wavelength 310 nm and FWHM 50 mm is used to collect the chemiluminescence signals from the exciated OH*

radicals. First, flame image photographs were obtained by the ICCD camera equipped with the bandpass filter centered at 310 nm are stored as a pixel array of (1024x1024). Then using Win-spec software the background image previously taken before experiment is subtracted. Then resulting image is an array of integers that are linearly scaled and then using Win-spec tools it is converted into ASCII file. By colour mechanism typical range of 8-bit image is usually [0, 255]. The maximum intensity at 255 is the saturated intensity and the maximum value of OH* intensity at tri-brachial point has been considered less than 255.

2.2 Monochromatic experiment

The collection wavelength of the chemiluminescence taken with ICCD camera might be broad. So the optical emission from these lifted flames is detected using a fibre optic based collection system coupled to JOBIN YVON THR-1000 high resolution monochromator (Asymmetric Czerny-Turner Configuration). To obtain an accurate measure of the total OH* and CH_2O* emission from the tri-brachial point of flame, the optical system used must be carefully designed. Moving system was used to move the burner in x and y-direction, and monochromatic system (Lens and Optic fiber) was fixed at constant position. In the present experiment, two optical lens of focal length 100 mm were used to obtain the constant signals at same height and to image the tri-brachial point of flame onto the end of 0.6 mm (600 um) diameter fused silica optical fiber. The light signals collected into the optical fiber was transported to the widely opened entrance slit of THR-1000 monochromator. The monochromator was used to identify the wavelength content of the light collected. Full wavelength scans in the

range of wavelengths between 3000A° to 6000A° and single wavelength measurement were performed. The intensity of the filtered light signal was measured using a photomultiplier tube (PMT) R-928. Both the diffraction grating and the PMT introduced known wavelength dependent losses. The measured voltages were corrected for these inefficiencies to obtain a true measure of the light intensity at a given wavelength in the light signal collected from the flame. Accumulations was set to 1000 and number of wavelength signals were averaged in the multiple of 0.4A°.

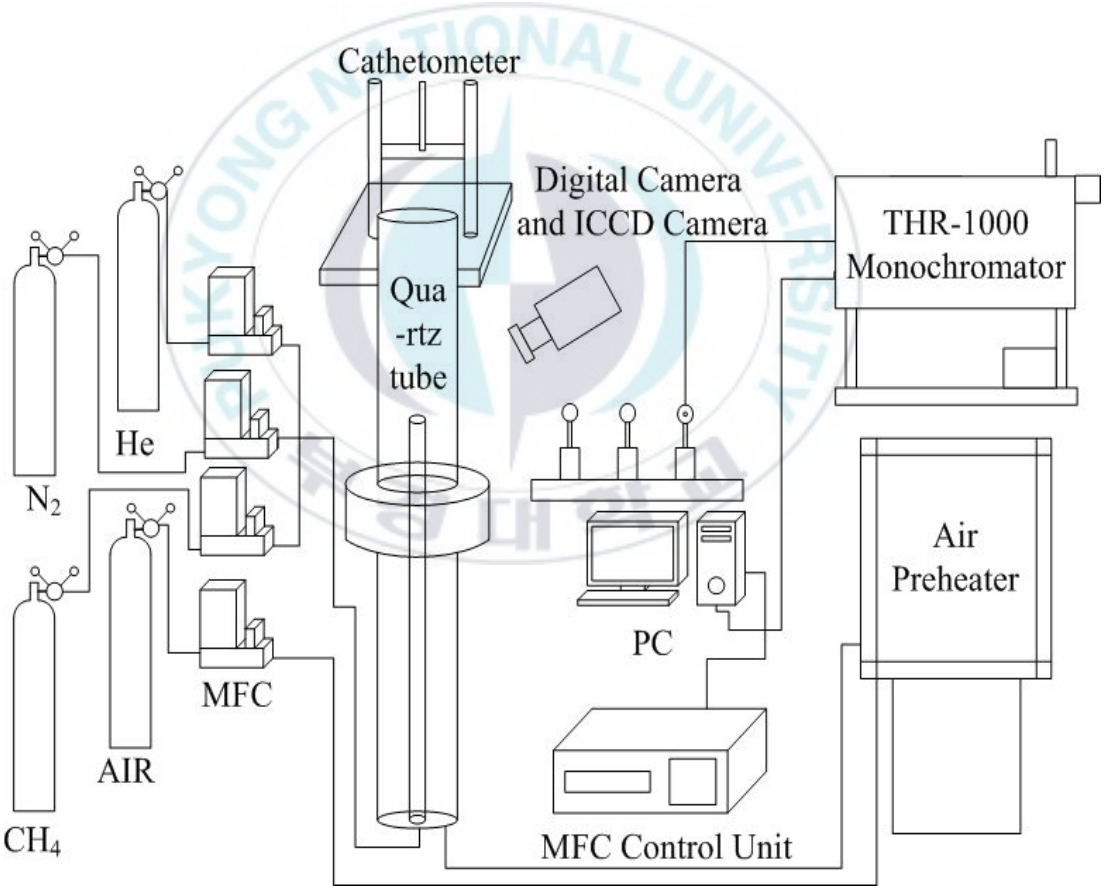

Fig. 1 Schematic diagram of experimental set-up

3. Results and Discussions

3.1 Stationary lifted flames

3.1.1 For methane diluted with helium (using 9.4 mm nozzle i.d.)

The experiments in methane jet flames were performed using 9.4 mm nozzle inner diameter co-flow burner with varying the initial fuel mole fraction $X_{F,O}$, fuel nozzle exit velocity, $U_{O.}$ Co-flow velocity $V_{CO,}$ was fixed to 10 cm/s. The variation of liftoff height, H_L with U_O at various $X_{F,O}$ for methane jet flames diluted with helium is shown in the Fig. 2(a). Overall, the liftoff heights increased nonlinearly with Uo, and were in the range of several millimeters to 123.7 mm. At Uo, 5 to 9 cm/s, lower than fixed co-flow velocity, such flames were reattached to the nozzle. Also, Fig. 2(b) shows the direct photographs of lifted flames at Uo = 14 cm/s for various $X_{F,O}$. Adding helium results in increase in the H_L with Uo until blowout occurs. For $0.2 < X_{F,O} < 0.34$, the flame was blown out and flame base became nearly flat for $5 < U\text{o} < 14$ cm/s. Flame flickering occurs near the tip region for Uo > 20 cm/s. Even with flickering, its influence on the liftoff height was negligible. Two distinct stabilization modes were observed in the developing and developed regions of laminar lifted nitrogen diluted propane co-flow jet flames [8]. For a reference, the developing region of free jet, Hfree was marked by dotted line. This was obtained to be H_{free}/d = 0.0165 X Re_d [19], where Re_d was the reynolds number defined as, Uod/v where v was the kinematic viscosity. Since the fuel is diluted, v was adopted with that of helium. The

variation in *H*free with *U*o is nearly linear as shown in the Fig. 2(a).

It was noted that lifted flames are observed at smaller nozle exit velocities less than stoichiometric un-stretched laminar flame speed and this was well depicted by buoyancy effect [20]. The influence of buoyancy was evaluated by the Richardson number as, $Ri = \rho gd/\rho U_o^2$, which was the ratio of the buoyancy induced momentum to the jet momentum, where g was the gravitational acceleration, ρ was the unburned density, and ρ was the density difference between unburned and burned gases. Richardson number was evaluated for *U*o = 5-30 cm/s at different stoichiometric conditions from $0.2 < X_{F,O} < 0.5$ is in the range of $0.8848 < Ri < 31.86$ as shown in the Fig. 2(a). The results shows that, buoyancy effect is more effective at low *U*o, (5-9 cm/s) with high *Ri* number and hence stationary lifted flames were observed. But with an increase in the *U*o, (10-30 cm/s) the value of *Ri* number is decreasing precipitously and buoyancy effect is suppressed significantly. Hence it was confirmed that, at low *U*o, in the developing region lifted flames are formed due to the effect of buoyancy but with an increase in the *U*o, influence of buoyancy goes to a minimum. Stationary lifted flames were observed in the co-flow jets for methane diluted with helium despite the *Sc* number is in the range of [$0.7 < Sc < 0.76$].

3.1.2 For methane diluted with helium (using 0.95 mm nozzle i.d.)

To obtain the lifted flames at much higher nozzle exit velocities than stoichiometric un-stretched laminar flame speed, experiments were conducted using 0.95 mm i.d. nozzle co-flow burner. Co-flow velocity *V*co, was fixed to 5 cm/s. The change in H_L with *U*o for methane diluted with helium at various

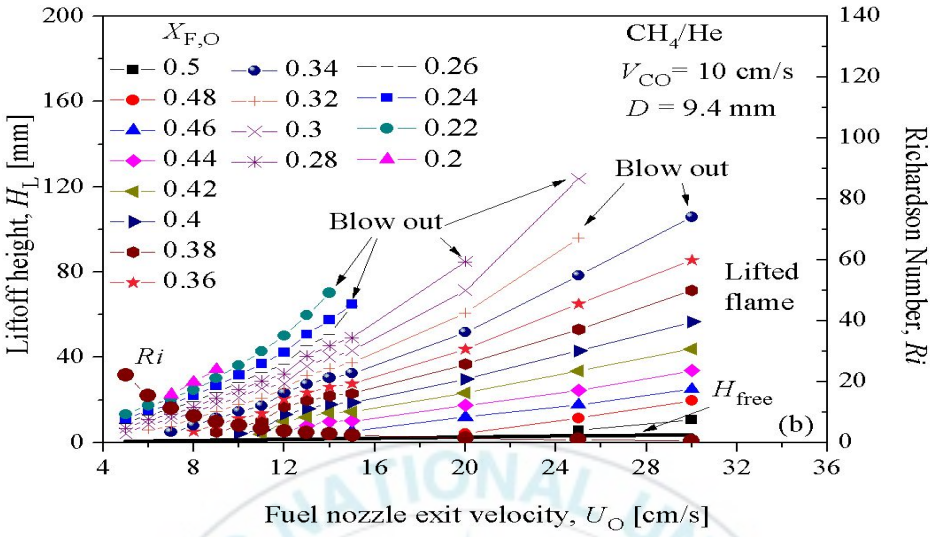

(a)

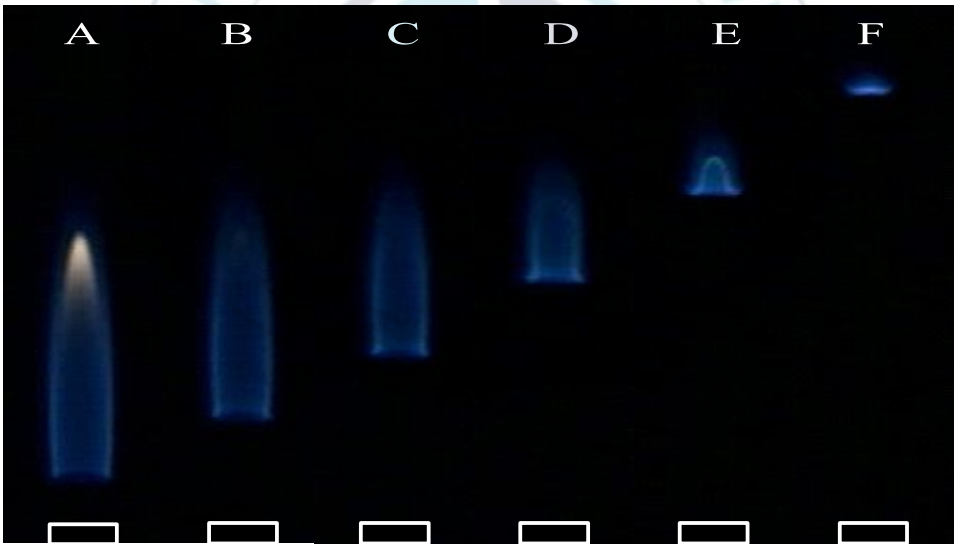

(b)

Fig. 2 (a) Change in liftoff height with fuel nozzle exit velocity for methane diluted with helium (Sc < 1) at various $X_{F,O}$ (b) direct photographs of stationary lifted methane jet flame diluted with helium for U_o = 14 cm/s, at (A) $X_{F,O}$ = 0.45 (B) 0.4 (C) 0.35 (D) 0.3 (E) 0.25 (F) 0.22.

$X_{F,O}$ is shown in the Fig 3(a). Liftoff height increases non-linearly by addition of helium diluent and with increase in the Uo. It is noted that, flame length increase with fuel nozzle exit velocity, Uo. Direct photographs of lifted flames for Uo = 260 cm/s at various $X_{F,O}$ are shown in the Fig. 3(b). Richardson number Ri, was also evaluated to observe the buoyancy effect and it is in the range of $0.00017 < Ri < 0.0015$. Results shows that, buoyancy effect can be suppressed with Uo, and lifted flames were obtained at higher Uo than stoichiometric un-stretched non-adiabatic laminar flame speeds despite the Sc number is in the range of $[0.69 < Sc < 0.72]$. The lifted flames obtained from two different nozzle diameter co-flow burners are plotted in a one graph.

Figure 4, shows the normalized liftoff height with Uo, considering stoichiometric un-stretched non-adiabatic laminar burning velocity for two different fuel nozzles 9.4 mm and 0.95 mm. Using 9.4 mm i.d. nozzle co-flow burner lifted flames are obtained at lower Uo than S_L^o and it is expressed as a buoyancy dominated regime. For 0.95 mm nozzle diameter lifted flames are obtained at higher Uo than S_L^o and it is expressed as a jet momentum dominated regime. The stoichiometric un-stretched non-adiabatic laminar burning velocities were evaluated by using oppdif code with detailed chemistry of GRI mechanism. This was because, the evaluation with adiabatic flame via Premixed code could not describe the effect of helium addition with high thermal conductivity. This un-stretched non-adiabatic stoichiometric laminar flame speed was achieved through extrapolation of the linear relation of flame speed versus global strain rate in a counterflow configuration. Figure 4, confirms that lifted flames exists for methane diluted with helium even at high Uo than S_L^o. For such cases, there are some other factors responsible for

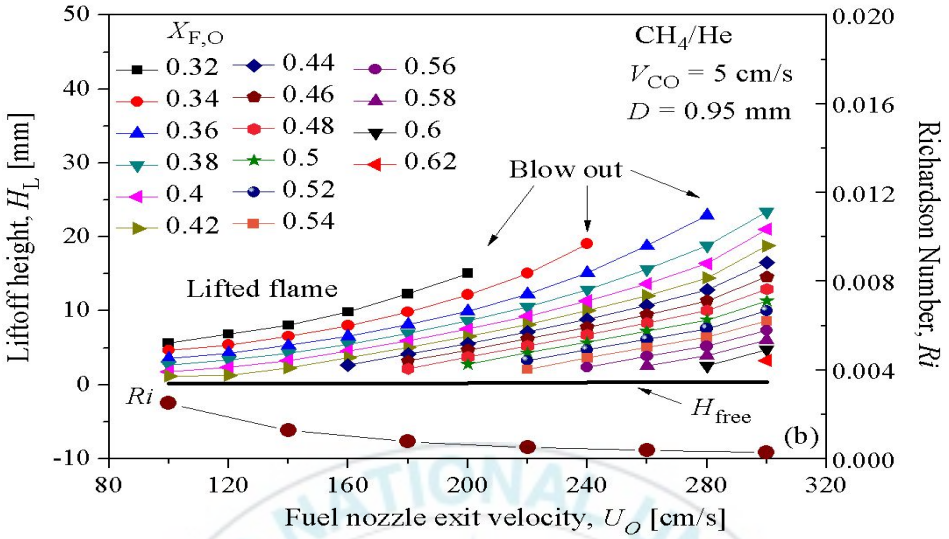

(a)

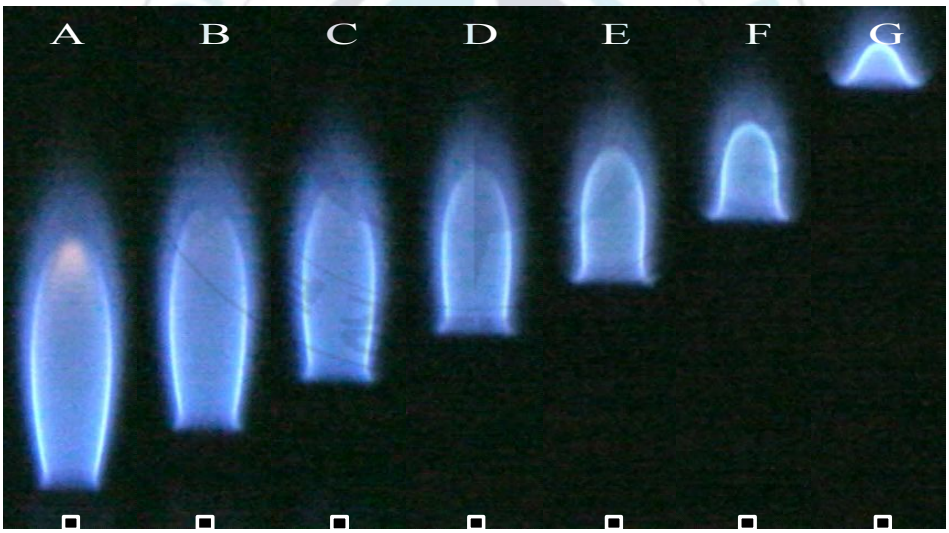

(b)

Fig. 3 (a) Change in liftoff height with fuel nozzle exit velocity for methane diluted with helium (Sc < 1) at various $X_{F,O}$ and (b) direct photographs of lifted methane jet flame diluted with helium for U_o = 260 cm/s, at (A) $X_{F,O}$ = 0.6 (B) 0.56 (C) 0.52 (D) 0.48 (E) 0.44 (F) 0.4 (G) 0.36

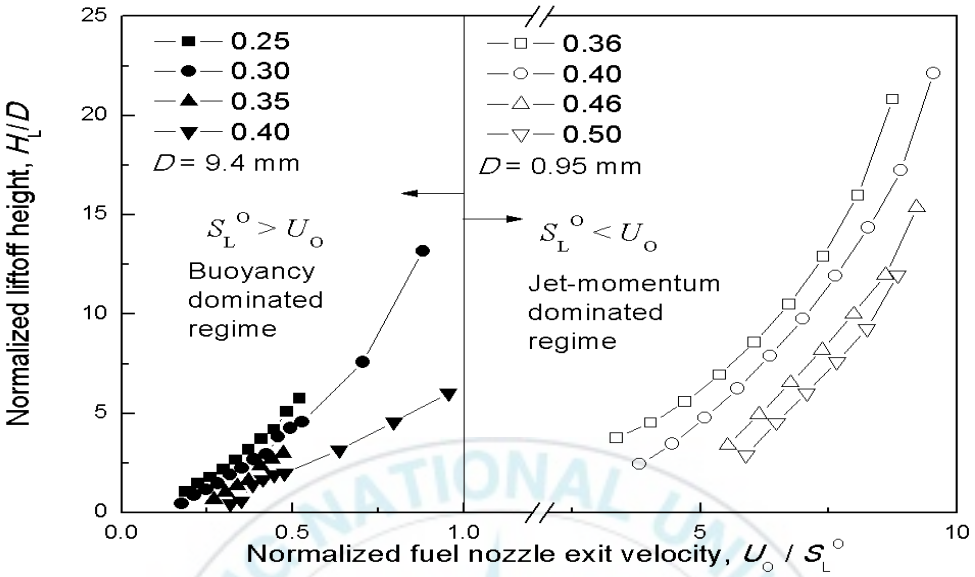

Fig. 4 Normalized liftoff height with fuel nozzle exit velocity considering stoichiometric un-stretched non-adiabatic laminar burning velocity for two different fuel nozzles.

flame stabilization will be discussed later.

The liftoff height in laminar lifted co-flow jet propane flames has been successfully described by the approximate similarity solution [21]. However, similarity solution in diluents added laminar lifted co-flow jet flames has yet to be developed. It is important to note that the similarity solution developed for laminar lifted free jet flames with a pure fuel has been successfully extended to diluents diluted laminar lifted free jet flames [21]. Based on this, similarity solution can be apply in the far field region of the lifted methane co-flow jet flames. Figure 5, shows the empirical characterization of the liftoff height with physical parameters, in the far-field region for 9.4 mm and 0.95 mm nozzle inner diameters, which corresponds to buoyancy and jet momentum

dominated regime. The characterized liftoff height increased with an increase in the Uo and decrease in $X_{F,O}$ as shown in the Fig.5 (a) and (b). The liftoff heights H_L, are described by the following:

$H_L = 2.31[(U_o/S_L^o) \times (1/X_{F,O})^{0.8}]^{1.84}$, with $R = 0.970$ at $V_{CO} = 10$ cm/s, for $D = 9.4$ mm

$H_L = 0.001[(U_o/S_L^o) \times (1/X_{F,O})^{0.8}]^{2.32}$, with $R = 0.974$ at $V_{CO} = 5$ cm/s, for $D = 0.95$ mm

where, R is the correlation coefficient.

3.1.3 For methane diluted with nitrogen (using 9.4 mm nozzle i.d.)

Liftoff of height variation with Uo at various $X_{F,O}$ for methane diluted with nitrogen is shown in the Fig. 6(a), and direct photographs of stationary lifted flames for Uo = 20 cm/s at different $X_{F,O}$ are shown in the Fig. 6(b). Although not shown clearly, flames edge has a tri-brachial structure, even though the lean premixed wing is somewhat obscure. This is because the edge is located near the nozzle where the mixture fraction gradient is expected to be large. The flame edge structure demonstrates the tri-brachial nature when H_L is large, while the nozzle attached flame edge shows that the lean premixed flame wing is merged to the diffusion flame, such that the bi-brachial structure is exhibited. Note that the flame length increases appreciably with Uo. Flame flickering occurs near the tip regin for Uo > 20 cm/s. Even with flickering its influence on the liftoff height was negligible.

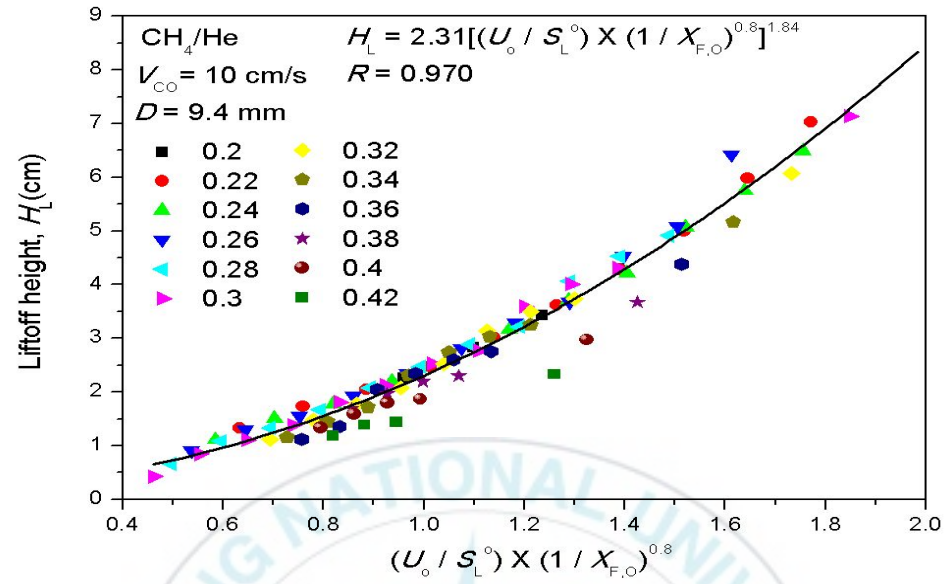

(a)

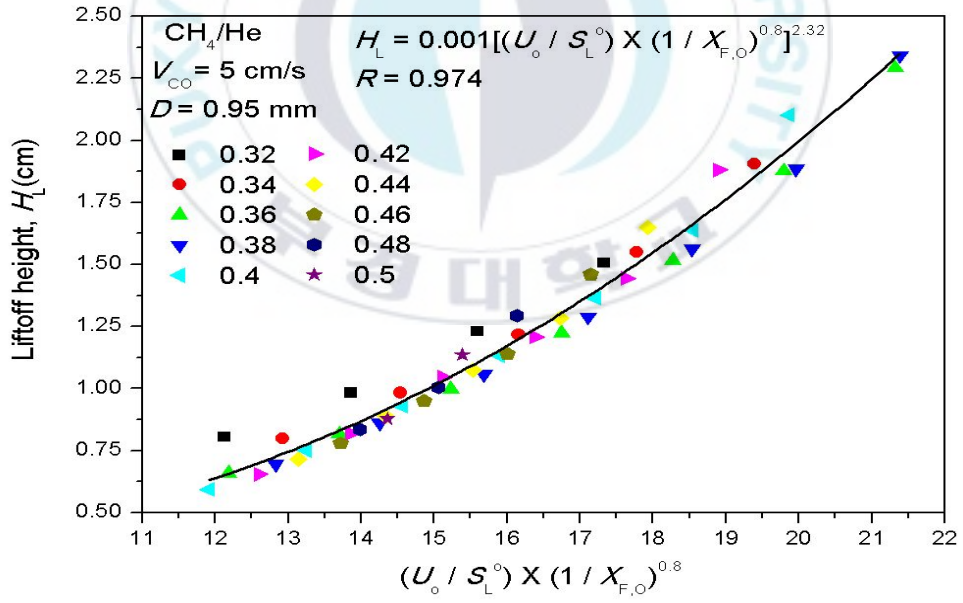

(b)

Fig. 5 Characterization of liftoff height in far field region for (a) 9.4 mm and (b) 0.95 mm nozzle inner diameters.

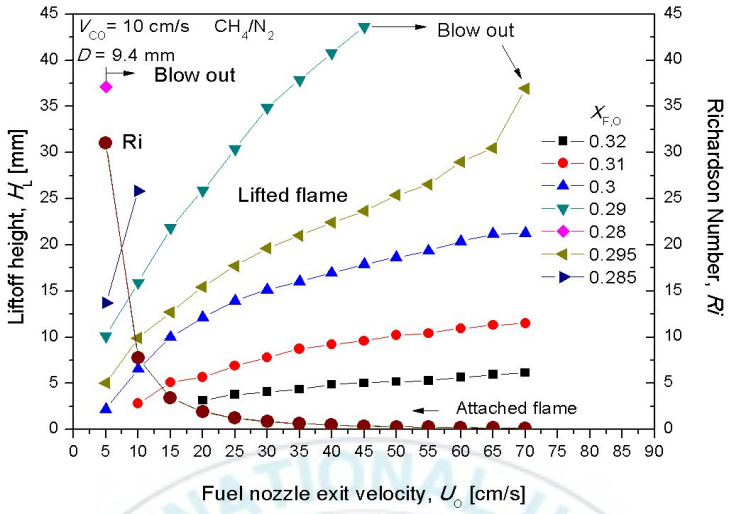

(a)

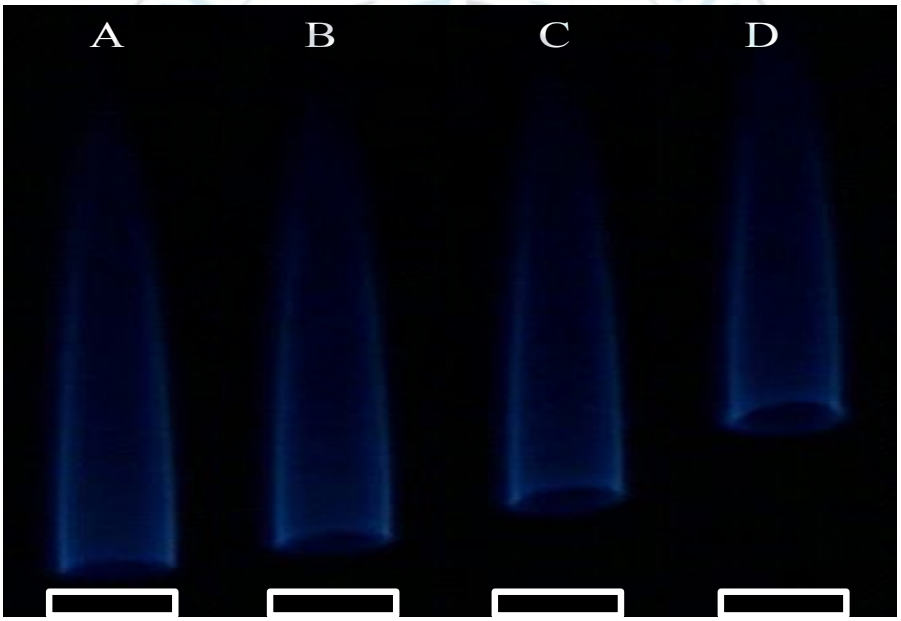

Fig. 6 (a) Change in liftoff height with fuel nozzle exit velocity for methane diluted with nitrogen (Sc < 1) at various fuel mole fractions and (b) direct photographs of stationary lifted methane jet flame diluted with nitrogen for U_o = 20 cm/s at (A) $X_{F,O}$ = 0.32 (B) 0.31 (C) 0.3 (D) 0.29.

The mechanism of flickering for non-premixed flames due to the Kelvin-Helmholtz instability [22] has been previously investigated. The blowout is observed at Uo = 40 cm/s for $X_{F,O}$ = 0.29. Stationary lifted flames were observed in the near field of co-flow jets for methane diluted nitrogen for Sc = 0.68. As discussed before, there were two different stabilization modes for the diluted propane [8] in the developing and developed regions of the co-flow jets. But for the methane diluted with nitrogen, stationary lifted flames are observed only in the developing region until blowout occurs.

This is consistent with the previous findings in the free jets that a lifted flame for methane having Sc < 1 is unstable and cannot be stabilized as stationary lifted flame in the developed region [1-2]. These lifted flames in the developing region are considered due to the influence of buoyancy at low Uo and this was checked by considering Ri number [20]. In the Fig. 6(a) the Ri number at various stoichiometric conditions for 0.29 < $X_{F,O}$ < 0.32 is in the range of 0.15 < Ri < 32.11. It shows that buoyancy effect is more influential at low Uo (5-20 cm/s) where Ri number is very large. Even if Ri number and hence buoyancy effect also decreased with the increased Uo, from (25-70 cm/s), stationary lifted flames are formed still in this region. To clarify the reason behind these lifted flames further investigations may require.

3.2 Stabilization of lifted flame

In previous discussions, lifted flames were observed for methane jet diluted with helium and nitrogen in buoyancy dominated and jet momentum dominated

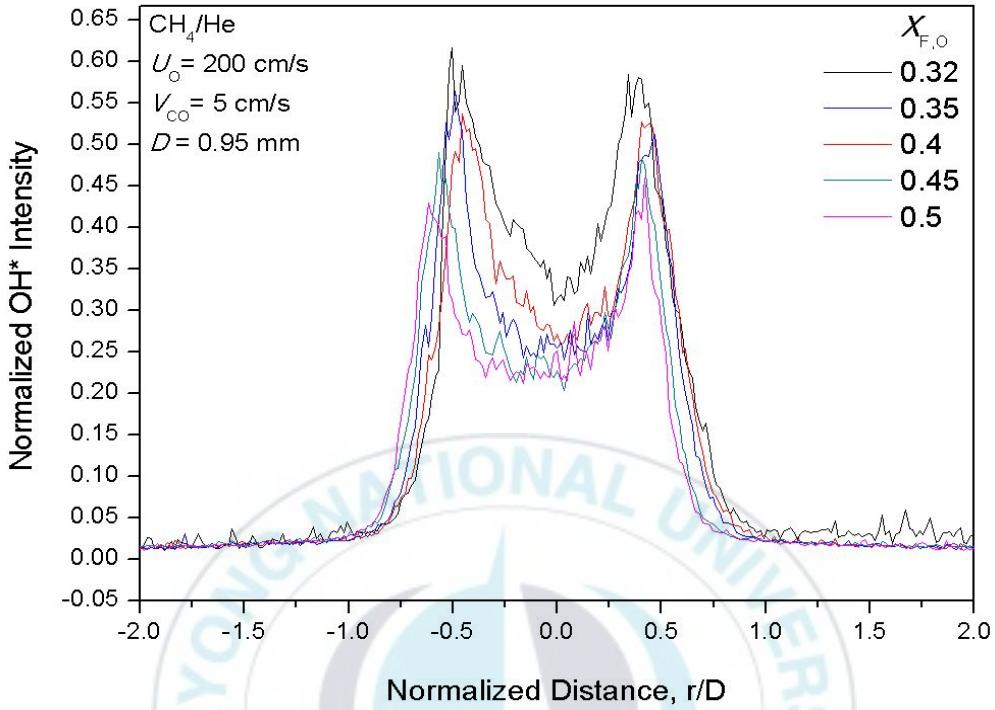

Fig. 7 Typical radial distribution of chemiluminescence intensity passing through the triple point at various $X_{F,O}$ for U_o = 200 cm/s and V_{co} = 5 cm/s in case of D = 0.95 mm.

regimes. So now how these lifted flames were stabilized in buoyancy dominated and jet momentum dominated regimes has to be addressed. It should be noted that, stabilization mechanism is still the balance of edge flame speed to the local flow one. This implies that, edge flame speed has to increase even with the mole fractions of helium and nitrogen and despite the reduction of mixture strength. To confirm it, flame images were captured by the intensified charge coupled device (ICCD) camera and chemiluminescence intensities of OH* radicals are measured at various conditions.

Typical radial distribution of OH* chemiluminescence intensity passing

through the tri-brachial point at Uo = 200 cm/s and various $X_{F,O}$ is shown in the Fig. 7, in case of D = 0.95 mm. The OH* chemiluminescence intensity have maxima at the triple points, indicating a double peak. We investigated the normalized maximum OH* intensity which was defined by the ratio of the OH* intensity at triple point to the saturated intensity. Based on them maximum OH* chemiluminescence intensities were examined at various $X_{F,O}$ and Uo. The measured OH* radical intensities for methane diluted with helium at Uo = 15 and 25 cm/s (which corresponds to buoyancy dominated regime) are shown in Fig. 8(a) and Fig. 8(b) shows OH* chemiluminescence intensities for methane diluted with nitrogen at Uo = 35 and 45 cm/s, at various $X_{F,O}$ using 9.4 mm nozzle inner diameter. The result shows that normalized maximum OH* intensities increased with increasing mole fractions of helium and nitrogen and decreased with fuel mole fraction. This implies that, buoyancy induced convection increases the reactant fluxes to the edge flame, increasing the reaction rate of edge flame and hence edge flame speed. Similar investigations were observed at Uo = 290 and 360 cm/s for D = 0.95 mm inner diameter nozzle as shown in Fig. 8(c). The normalized maximum OH* intensity increases with helium mole fractions as well. For such a high nozzle exit velocity, Richardson number is negligible. Then buoyancy effect may not explain such tendency, meaning that there are some another reasons.

Chemiluminescence intensities of OH* and CH_2O* were also measured using monochromatic experiment. A typical spectral wavelength scan of the lifted flame at tribrachial point is shown in Fig. 9, for Uo = 360 cm/s and $X_{F,O}$ = 0.6. The spectrum shows peaks of four major chemiluminescence species OH*, CH_2O*, CH* and C_2*. To obtain the peak intensity of chemiluminescence,

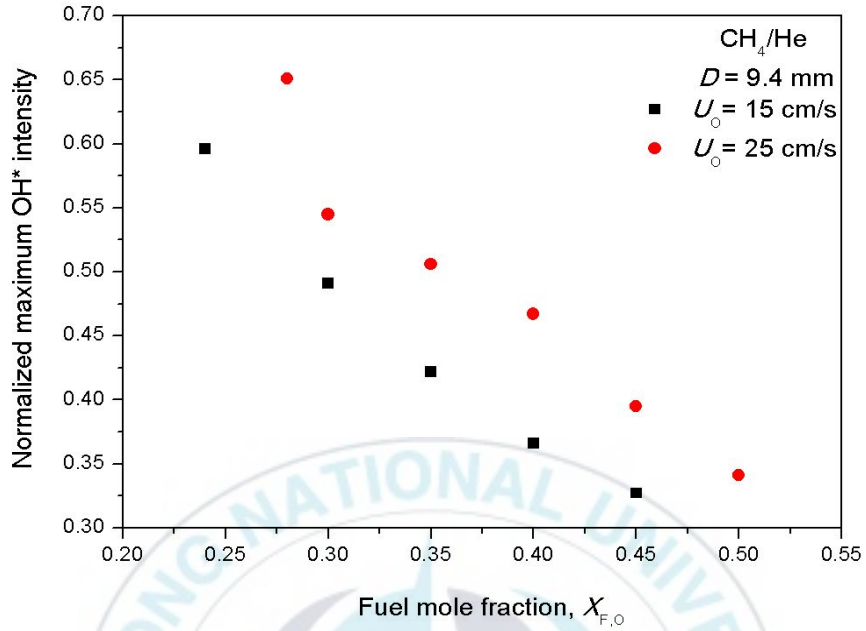
CH4/He
D = 9.4 mm
UO = 15 cm/s
UO = 25 cm/s
Normalized maximum OH* intensity
Fuel mole fraction, XF,O
0.70
0.65
0.60
0.55
0.50
0.45
0.40
0.35
0.30
0.20
0.25
0.30
0.35
0.40
0.45
0.50
0.55

(a)

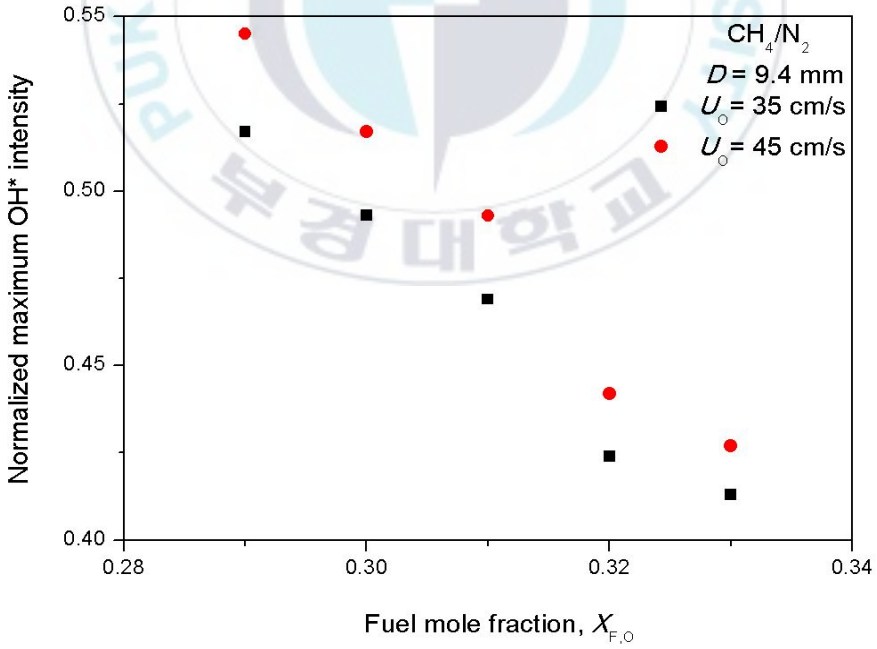
CH4/N2
D = 9.4 mm
UO = 35 cm/s
UO = 45 cm/s
Normalized maximum OH* intensity
Fuel mole fraction, XF,O
0.55
0.50
0.45
0.40
0.28
0.30
0.32
0.34

(b)

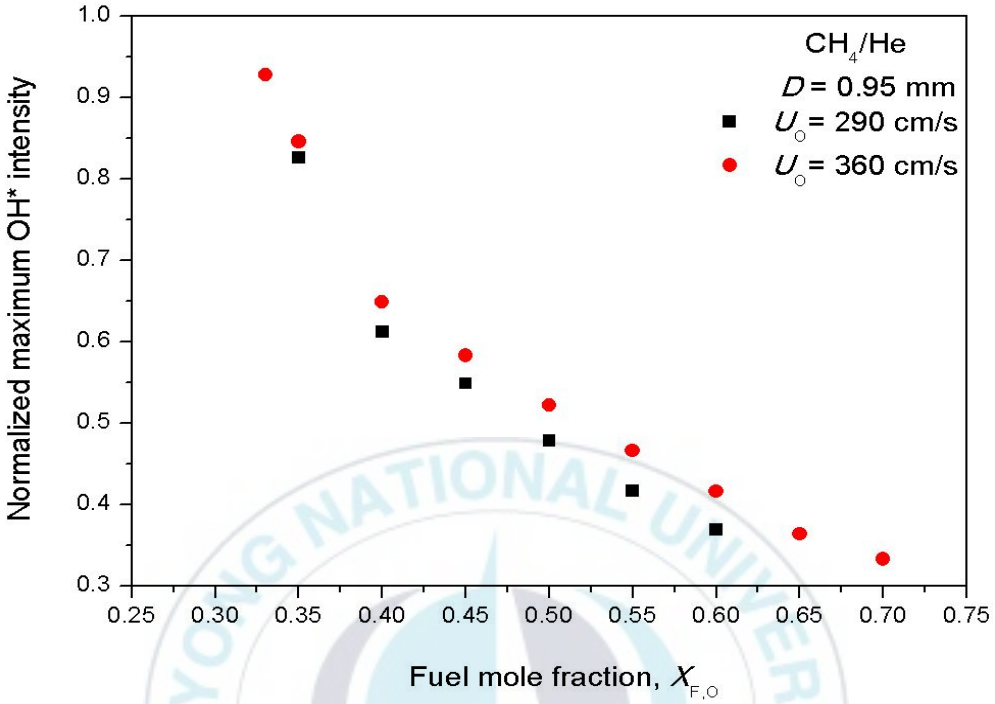

(c)

Fig. 8 Measured OH^* radical intensities for (a) methane diluted with helium at U_o = 15 and 25 cm/s and (b) methane diluted with nitrogen at U_o = 35 and 45 cm/s, for various $X_{F,O}$ using 9.4 mm nozzle diameter (c) for methane diluted with helium at U_o = 290 and 360 cm/s and various $X_{F,O}$ using 0.95 mm nozzle diameter.

number of wavelength were averaged in the multiple of 0.4A°. the peak intensities of OH* and CH_2O* chemiluminescence were obtained at 3088A and 3908A respectively after the subtraction of background emission of light spectrum with optic fiber in the same range of wavelength. The total wavelengths obtained only represents the portion of light collected by the lens system and not that lost in transfer from lens to fiber or fiber to monochromator.

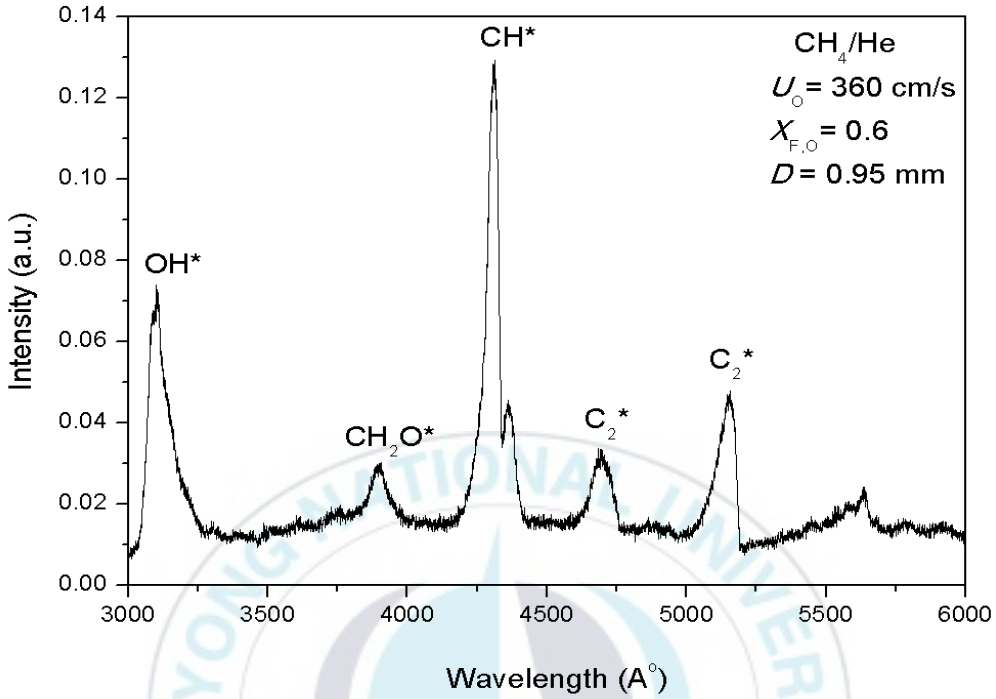

Fig. 9 Spectral wavelength scan of the lifted flame

However, the measurement system does not discriminate with respect to the location of the origin of the light lost and so the measurement is a true representation of the total OH* and CH_2O* chemiluminescence from the tri-brachial point of the lifted flame.

Figure 10(a), shows the measured OH* chemiluminescence scanned area with increase in the $X_{F,O}$ for methane diluted with helium at Uo = 290 and 360 cm/s using D = 0.95 mm nozzle inner diameter. Similar investigations were observed for monochromatic experiment as with the ICCD camera, OH* chemiluminescence intensities were decreased with $X_{F,O}$ and increased with helium diluent mole fractions. Also, the use of product of [OH] X [CH_2O] as a marker for heat release rate was validated in previous studies [14]. So we

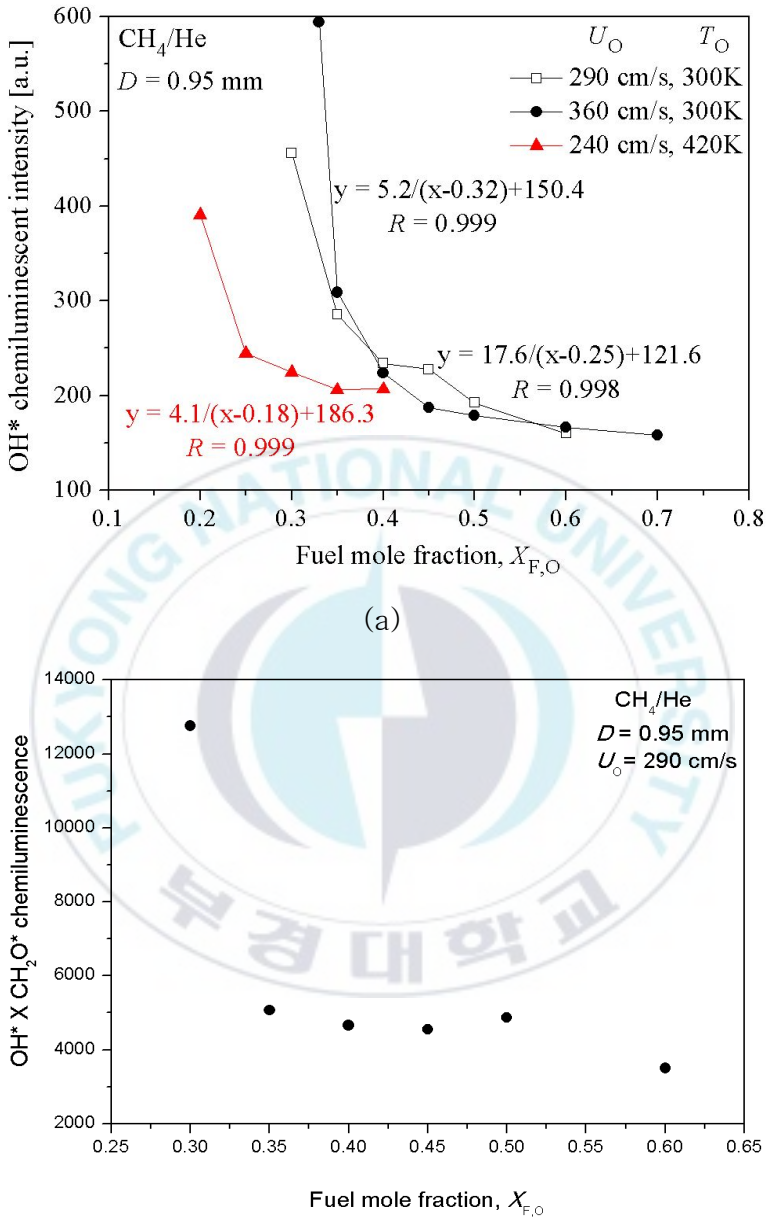

Fig. 10 (a) Measured OH^* chemiluminescence intensity using monochromatic experiment (b) Product of [OH] X [CH2O] as marker for heat release rate, with increase in the $X_{F,O}$.

measured the product of OH* and CH_2O* as shown in the Fig. 10(b) at Uo = 290 cm/s, which shows the decreasing behavior with $X_{F,O}$. It implies that, an increase in the reaction rate and hence edge flame speed with the enhancement of chemiluminescence intensities.

Although it is not provided that, at a fixed strain rate in a counterflow configuration, OH* concentration decreases with diluents mole fraction of He and N_2. Then enhancement of edge flame speed through chemical effects is not plausible in reasoning such phenomena. Nevertheless, the feasibility in high temperature ambience will remain in future work because the stabilization mechanism has a jump from the balance of edge flame speed to the local flow speed at normal temperature ambience to reduction in ignition delay time at high temperature ambience. Also edge flame speed has the dependancy upon the mixture strength, buoyancy, fuel concentration gradient (strain rate and thereby radius of curvature), and Lewis number. Because mixture strength decreases with diluent addition, it has a negative effect in flame stabilization. The range of the Lewis number is 1.08~1.36(0.963~0.964) for helium (nitrogen) addition (both decrease with fuel mole fraction), respectively. Particularly, for helium addition, it has a negative effect on edge flame speed such that, the Lewis number increases with helium mole fraction. This means that, effect of Lewis number cannot be a main reason of flame stabilization. Thus important role on edge flame speed enhancement may be addressed to radius of curvature Figure 11, shows the appreciable increase in r^*_{cur}, with helium mole fraction in jet momentum dominated regime, thereby increasing edge flame speed. In such manner, lifted flame stabilization for methane jet could be explained based on the stabilization mechanism.

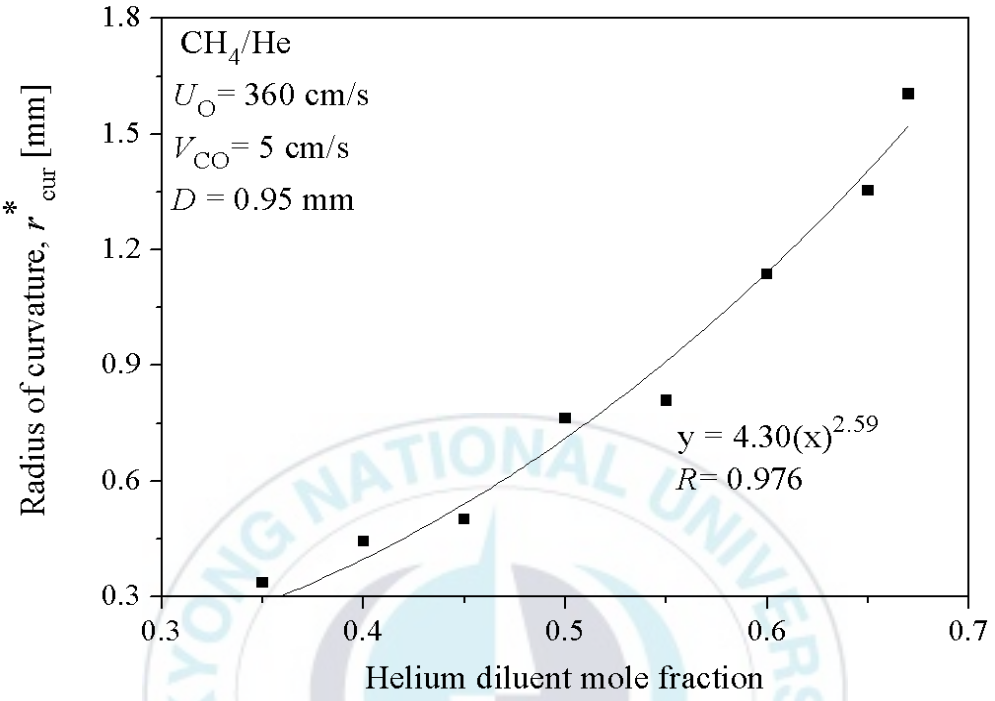

Fig. 11 Radius of curvature r^*_{cur}, of lifted methane jet flame with the addition of helium dilution by using 0.95 mm nozzle diameter.

4. Conclusion

Stabilization mechanism of laminar lifted methane jet flame diluted with helium and nitrogen having (Sc < 1) has been investigated experimentally. For 9.4 mm nozzle inner diameter lifted flames existed at $U_o < S_L^o$. Based on stabilization mechanism, the stabilization of lifted flames were caused by buoyancy induced convection flow such that it could increase the reactant mass fluxes to edge flame (increasing the reaction rate and edge flame speed). However even in jet momentum dominated regime (experimented with D = 0.95 mm nozzle i.d.) lifted methane jet flames diluted with helium existed at ambient temperature. It was found that, in such lifted flames an appreciable increase of radius of curvature in addition to increased OH* and CH_2O* concentration contributed to the flame stabilization.

Acknowledgement

It is indeed a great pleasure and sense of fulfillment for me to present a thesis report on

“Laminar Lifted Methane Jet Flames in Co-flow Air Diluted with Helium and Nitrogen”

I regard myself to be most fortunate to get an opportunity to work under the versatile and kind guidance of Prof. Jeong Park. I acknowledge a deep sense of guidance for their constant inspiration and helpful criticism.

I also thankful to our senior and older brother Mr. Won June Lee, all laboratory members for their kindness and providing necessary inputs at the right time.

Last but not least, no words enough to express heartiest gratitude to our beloved parents Mr. Pandurang Sapkal and Mrs. Hirabai Sapkal for their assistance in building up my carrier.

Thanking in anticipation all readers.

Sincerely,

Narayan Pandurang Sapkal

References

[1] S.H. Chung, B.J. Lee, On the characteristics of laminar lifted flames in a non-premixed jet. Combust. Flame 86 (1991) 62-72.

[2] B.J. Lee, S.H. Chung, Stabilization of lifted tri-brachial flames in a laminar non-premixed jet. Combust. Flame 109 (1997) 163-172.

[3] Y.S. Ko, S.H. Chung, Propagation of unsteady tri-brachial flames in laminar non-premixed jets. Combust. Flame 118 (1999), 151-163.

[4] Y.S. Ko, S.H. G.S. Kim, S.W. Kim, Stoichiometry at the leading edge of a tri-brachial flame in laminar jets from Raman scattering technique, Combust. Flame 123 (2000) 430-433.

[5] J. Lee, S.H. Won, S.H. Jin, S.H. Chung, O. Fujita, K. Ito, Propagation speed of tri-brachial flame of propane in laminar jets under normal and micro gravity conditions, Combust. Flame 134 (2003) 411-420.

[6] Ruetsch G.R., Vervisch L., and Linan A., Phys. Fluids 7:1447-1454 (1995).

[7] J.Y. Chen, T. Echekki, Numerical study of buoyancy and differential diffusion effects on the structure and dynamics of triple flames, Combust. Theory Mod. 5(2001) 499-515.

[8] S.H. Won, S.H. Chung, M.S. Cha and B.J. Lee, Lifted flame stabilization in developing and developed regions of co-flow jets for highly diluted

propane. Proc. Combust. Inst. 28 (2000) 2093-2099.

[9] M.D. Smoke, A. Ern, M.A. Tanoff, B.A. Valdati, R.K. Mohammed, D.F. Marran, M.B. Long, Proc. Combust. Inst. 26 (1996) 2161-2170.

[10] X. Qin, I.K. Puri, S.K. Agarwal, Characteristics of lifted triple flames stabilized in the near field of a partially premixed axisymmetric jet, Proc. Combust. Inst. 29 (2002) 1565-1572.

[11] T. Plessing, P. Terhoeven, N. Peters, An experimental and numerical study of a laminar triple flame, Combust. Flame 115 (1998) 335-353.

[12] Paul R. Medwell, David L. Blunck, Bassam B. Dally, The role of precursors on the stabilization of jet flames issuing into a hot environment. Combust. Flame 161 (2014) 465-474.

[13] R.L. Gordon, A.R. Masri, E. Mastorkos, Simultaneous rayleigh temperature, OH and CH2O-LIF imaging of methane jets in a vitiated coflow, Combust. Flame 155 (2008), 181-195.

[14] P.H. Paul, and H.N. Najm, Proc. Combust. Inst. 27 (1998), 43-50.

[15] A. Fayoux, K. Zahringer, O. Gicquel, J.C. Rolon, Experimental and numerical determination of heat release in counterflow premixed laminar flames, Proc. Combust. Inst. 30(2005) 251-257.

[16] S.B. Dworkin, A.M. Schaffer, B.C. Connelly, M.B. Long, M.D. Smooke, M.A. Puccio, B. McAndrew and J.H. Miller, Proc. Combust. Inst. 32(2009), 1311-1318.

[17] Robert L. Gordon, Assaad R. Masri, E. Mastorakos, Heat release rate as represented by [OH] X [CH2O] and its role in autoignition, Combust. Theory Mod. 13 (2009) 645-670.

[18] S.H. Chung, Stabilization, propagation and instability of tri-brachial flame, Proc. Combust. Inst.31 (2007) 877-892.

[19] Lee D.S., S.H. Chung and K.D. Kim, J. Fluid Engin. Trans. ASME, 119:716-718, (1997).

[20] S.H. Won, J. Kim, K.J. Hong, M.S. Cha, S.H. Chung, Stabilization mechanism of lifted flame edge in the near field of co-flow jets for diluted methane. Proc. Combust.Inst. 30 (2005) 339-347.

[21] S.H. Won, S.H. Chung, M.S. Cha and B.J. Lee, Lifted flame stabilization in developing and developed regions of co-flow jets for highly diluted propane. Proc. Combust. Inst. 28 (2000) 2093-2099.

[22] J. Buckmaster, N. Peters, The infinite candle and its stability: A paradigm for flickering diffusion flames, Proc. Combust. Inst. 21 (1986) 1829-1836.